Available online at www.sciencedirect.com
SCIENCE DIRECT®
Cement & Concrete Composites 27 (2005) 809–817
Cement & Concrete Composites
www.elsevier.com/locate/cemconcomp

Field monitoring of electrical conductivity of cover-zone concrete

W.J. McCarter [a,*], T.M. Chrisp [a], G. Starrs [a], P.A.M. Basheer [b], J. Blewett [c]

[a] School of the Built Environment, Heriot-Watt University, Edinburgh, EH14 4AS Scotland, UK
[b] School of Civil Engineering, Queen's University, Belfast, BT7 1NN Northern Ireland, UK
[c] Mott MacDonald Ltd., Consulting Engineers, Edinburgh, EH6 7EZ Scotland, UK

Received 19 July 2004; accepted 8 March 2005

Abstract

A sensor system, developed in a previous laboratory study [McCarter WJ, Emerson M, Ezirim H. Properties of concrete in the cover-zone: developments in monitoring techniques. Mag Conc Res 1995;47(172):243–51; Chrisp TM, McCarter WJ, Starrs G, Basheer PAM, Blewett J. Depth related variation in conductivity to study wetting and drying of cover-zone concrete. Cem Conc Comp 2002;24(5):415–27], is used to obtain the spatial distribution of electrical conductivity within the cover-zone of concrete specimens subjected to a range of natural exposure conditions. The testing methodology enables in-situ monitoring of the electrical conductivity and technical issues relating to site measurements are discussed. The work also highlights the need for continual monitoring of the covercrete as the electrical conductivity changes with time, depth and environment.

Keywords: Concrete; Cover-zone; Durability; Field monitoring; Electrical conductivity

1. Introduction

The major part of the European infrastructure has reached an age where capital costs have decreased, but inspection and maintenance costs have grown to such an extent that they now constitute a major part of the recurrent costs of the infrastructure. Traffic delay costs due to inspection and maintenance programmes are already estimated to be between 15% and 40% of the construction costs [3]. The development of integrated monitoring systems for new and existing reinforced concrete structures could reduce costs by allowing a more rational approach to the assessment of repair options and scheduling of inspection and maintenance programmes, thereby minimising traffic delays resulting from road closures. The ability to continuously monitor cover-zone concrete (covercrete)—*in real time*—could also allow a more informed assessment of the current and future performance of the cover-zone. The development of sensor systems to assess covercrete performance and durability forms one important component of an overall integrated monitoring system.

It is now recognised that in the total management of structures, which involves both whole-life economics and life-cycle calculations [4,5], integrated monitoring systems and procedures have an important role to play [6]. When data from monitoring systems are used with improved service-life prediction models [7,8] additional savings in life cycle costs could result. Satisfactory guidelines for concrete durability can only be developed by monitoring covercrete performance under a range of exposure conditions, over an extended period of time. Indeed, performance-based specifications for concrete are now defined in EN 206-1: 2000 (Annex J) [9] and may be more appropriate than a prescriptive *deem-to-satisfy* approach.

There are three broad levels of monitoring [10] designated: high, medium and low and the appropriate level of monitoring must be considered at the design stage.

* Corresponding author. Tel.: +44 0131 451 3318; fax: +44 0131 451 4617.
E-mail address: w.j.mccarter@hw.ac.uk (W.J. McCarter).

0958-9465/$ - see front matter © 2005 Elsevier Ltd. All rights reserved.
doi:10.1016/j.cemconcomp.2005.03.008

As part of a high-level programme, the installation of sensors within the covercrete would be considered. This current work focuses on a sensor arrangement that allows electrical measurements to be taken within the covercrete. Such measurements are technically simple to obtain and can be presented in a range of formalisms to allow ease of data interpretation.

2. Covercrete sensors

The primary function of covercrete sensor systems is to provide real-time data on the condition of the covercrete and the spatial distribution of cover-zone properties. A number of sensor systems allow monitoring of the electrical properties of the concrete and/or steel at discrete distances from the exposed surface. For example, Schießl's ladder [6,10,11] represents a system whereby mild steel (m/s) anodes are embedded at discrete points within the cover region. Macrocell current flow is measured between each m/s anode and a stainless steel cathode; the current flow through the elements is used to follow the depassivation front through the cover-zone.

In order to study water, ionic and moisture movement within the surface zone, two systems are noteworthy—a multi-ring electrode moisture sensor [6,11] and a covercrete electrode-array developed by the authors [1]. Both systems allow discretised electrical measurements to be taken within the concrete cover-zone, although the electrode geometry and layout is significantly different in both systems. The current work focuses on the covercrete electrode array used and detailed in previous laboratory-based studies [1,2]. In summary, the sensor comprises 10 electrode pairs mounted on a small plexiglas former. Each electrode comprises a stainless steel pin (1.2 mm in diameter) which was sleeved to expose a 5 mm tip; in each electrode pair the pins had a (horizontal) centre to centre spacing of 5 mm. The pairs of electrodes were then arranged vertically at 5 mm intervals thus enabling electrical measurements to be taken at 10 discrete points over a depth of 50 mm. In addition, the electrode pairs were off-set from each other in both the horizontal and vertical directions; also, the exposed tip of the electrode was positioned remote from the plexiglas former (>maximum aggregate size + 5 mm). Four thermistors, positioned at 10, 20, 30 and 40 mm from the exposed surface, were also mounted on the sensor thereby enabling temperature profiles to be obtained within this region.

3. Experimental programme

For the current work, results are presented from concrete samples exposed to the following environmental conditions:

1. A marine environment with samples positioned vertically in galvanised steel frames at three locations—above high water mark (denoted high-level: see Fig. 1(a)), just below high water-mark (denoted

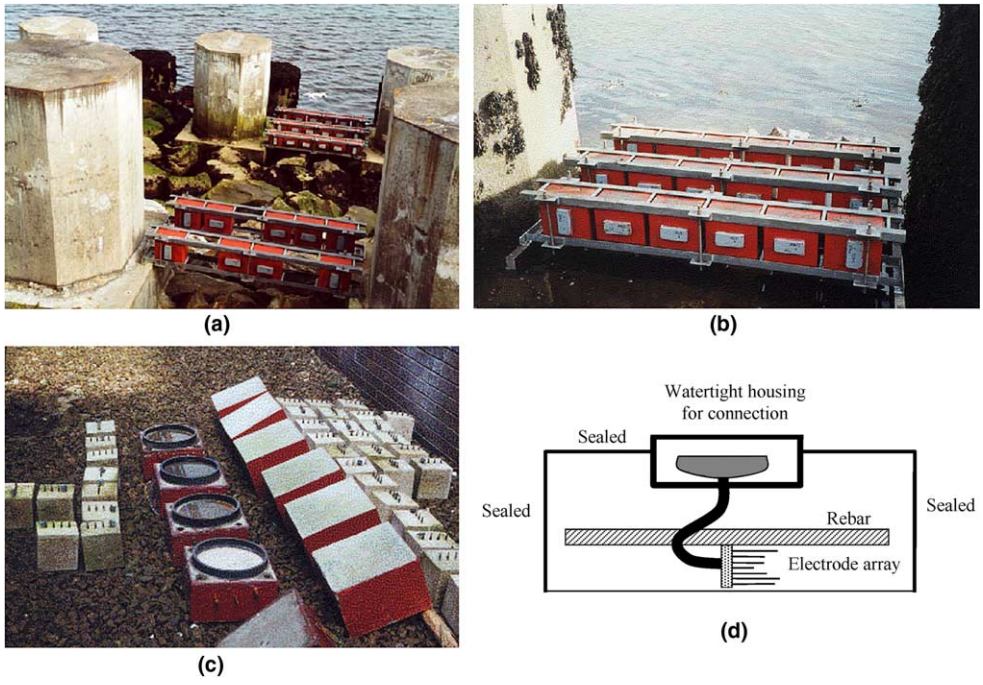

Fig. 1. (a) Marine exposure site showing specimens at high-level (foreground) and mid-level (centre) positions; (b) marine exposure site showing specimens at the low-level position; (c) urban exposure site showing six (of nine) test specimens; and (d) schematic showing termination of cabling from sensor and thermistors in water-tight housing at back face of specimens.

mid-level: see Fig 1(a)) and just above low-water mark (denoted low-level: see Fig. 1(b)). These are classified as, respectively, exposure classes XS1, XS3 and XS2 as defined in [9]; in addition, the exposed face of all samples was facing in a north-easterly direction.

2. An urban environment with specimens positioned in an open gravel yard close to the north side of a three-storey building. This would be equivalent to exposure class XC4/XF1 as defined in [9]. The exposed face of the specimens was north-facing and the specimens, themselves, were inclined (Fig. 1(c)).

The cements used were Portland cement (PC), PC blended with granulated blast-furnace slag (GGBS) and PC blended with pulverised fuel ash (PFA) designated, respectively, CEM I 42.5N, CEM III/A 42.5N and CEM II/B-V 42.5N by EN 197-1 [12]. Table 1 presents the mix details together with the mean 7- and 28-day compressive strength determined on 100 mm cubes (denoted F_7 and F_{28}); a gravel aggregate and washed concreting fines were used throughout. The oxide composition of the cementitious materials is presented in Table 2; the PFA conformed to BS3892 [13] and GGBS to BS6699 [14]. The concretes detailed in Table 1 represent mixes used in current practice.

For both sites, samples took the form of $300 \times 300 \times 200$ mm (depth) blocks cast in plywood formwork, which had been given coat of proprietary release agent (Nuffins Formstrike) prior to casting. A covercrete electrode array was secured within the surface zone and at the centre of the 'working face' of each sample (i.e. the 300×300 mm face cast against the formwork). The blocks were lightly reinforced with two, 16 mm diameter rebars (200 mm in length) which had a 50 mm cover from both the working face and side faces. Cabling from the electrodes and thermistors was taken into a watertight glass reinforced plastic box cast into the face opposite to the working face (see schematic in Fig. 1(d)). After demoulding at 24 h, the samples were wrapped in damp hessian and stored under polythene tentage for a total of seven days; after this time the polythene and hessian were removed and the specimens left in the laboratory (15–20 °C, 55 ± 5%RH). All specimens were then sealed on five faces with two coats of a high-build epoxy coating, with the working face left unsealed. A total of 54 samples were cast and deployed as follows:

(i) *Marine site:* six samples of each mix in Table 1 were placed at the low- and mid-level locations;
(ii) *Marine site:* three samples of each mix placed at the high-level location; and
(iii) *Urban site:* three samples of each mix.

Approximately 4-weeks after demoulding, the concrete blocks were transported to the marine site and placed in position during the month of February. The specimens were saturated with water prior to placement which prevented excessive absorption of seawater initially. Samples for the urban site were left in the laboratory for approximately 20 weeks after demoulding before being placed outside during the month of June (these samples were not saturated prior to placement).

3.1. Calibration and data logging

To allow the measured electrical resistance (R, in Ω) of the concrete to be converted to conductivity (σ, in Siemens/m, S/m), the covercrete array had to be calibrated in solutions of known conductivity prior to installation. Having obtained the calibration constant for the electrode pairs (denoted k), the conductivity, σ of the material between the electrodes (or its reciprocal resistivity, ρ (Ω m)) is given by,

$$\sigma = \frac{k}{R} = 1/\rho \tag{1}$$

As the array comprised ten electrode pairs, an average value of k was evaluated for the sensor to give an overall sensor constant. The value of k was obtained from

Table 1
Concrete mixes used in the testing programme (Plast. = plasticiser (Sika FR); *w/b* = water–binder ratio)

Mix designation	Mix ref.	PC (kg/m^3)	PFA (kg/m^3)	GGBS (kg/m^3)	20 mm (kg/m^3)	10 mm (kg/m^3)	Fines (kg/m^3)	Plast. (l/m^3)	*w/b*	Slump (mm)	F_7 (MPa)	F_{28} (MPa)
CEM I 42.5N	PC	460	–	–	700	350	700	1.84	0.4	105	57	70
CEM III/A 42.5N	GGBS	270	–	180	700	375	745	3.60	0.44	140	31	53
CEM II/B-V 42.5N	PFA	370	160	–	695	345	635	2.65	0.39	110	33	58

Table 2
Oxide analysis of cementitious materials (wt.%)

Oxide	SiO_2	Al_2O_3	Fe_2O_3	CaO	MgO	SO_3	K_2O	Na_2O
PC	20.68	4.83	3.17	63.95	2.53	2.80	0.54	0.08
GGBS	32.53	13.78	0.37	41.27	6.63	1.18	0.55	0.26
PFA	53.08	30.14	7.20	1.68	2.50	0.20	0.41	0.30

laboratory tests by placing the sensor in liquids of known conductivity; the conductivity of these liquids was varied over a wide range, which included the range of values anticipated in the field. A value of $k = 80\ \mathrm{m}^{-1}$ (±5%) was obtained for the sensors used in the current work. Changes in resistance between pairs of electrodes (made parallel to the exposed surface) were measured using an auto-ranging impedance analyser (Hewlett Packard 4263B LCR meter) interfaced to a multiplexing switch control unit (Hewlett Packard 34970A). The system was controlled by a laptop using HPVEE software. Preliminary studies indicated that an alternating current (a.c.) operating at a frequency of 1 kHz and signal amplitude of 1 V would ensure electrode polarisation effects are reduced to a minimum [15]. Thermistor measurements were also logged using the same system. The data acquisition system was contained within a weathertight case and powered by a small portable generator.

4. Results and discussion

The primary objective of this current work is to extend the previous laboratory-based studies, which used controlled cycles of wetting and drying, to samples exposed to natural environments. Data are presented for the initial 800 days exposure. Regarding electrical measurements, a number of presentation formats are used,

(i) the variation of conductivity measurements standardised to a reference temperature, σ_t, which was 20 °C in this instance (see below);
(ii) variation of *normalised* conductivity using the values in (i) above where the normalised conductivity, N_c, is defined as,

$$N_c = \frac{\sigma_t}{\sigma_0} \tag{2}$$

σ_t is the standardised conductivity measured at a particular electrode position on the sensor at time, t, and σ_0 and is the initial (standardised) value of conductivity (i.e. at placement) across the particular electrode pair;
(iii) N_c, or conductivity, profiles through the covercrete, i.e. the variation in these parameters with depth through the cover.

4.1. Temperature effects on electrical measurements

Concrete exposed to the natural environment will be subjected to temperature variations and its electrical conductivity will fluctuate in sympathy with the concrete temperature. When undertaking electrical measurements on concrete it is desirable to distinguish between changes in conductivity due to changing levels of pore saturation and/or ionic concentration within the pore-fluid and changes in conductivity due to changes in ambient temperature. To compensate for this effect, concrete conductivity measurements can be *standardised* to an equivalent conductivity at a predefined reference temperature through the application of a temperature correction formula. For example, the following formula, which is applicable to electrolytic solutions, has been used to quantify the effect of temperature on concrete conductivity [16–18]:

$$\sigma_T = \frac{\sigma_\theta}{[1 + \alpha(\theta - T)]} \tag{3}$$

where σ_T is the conductivity of the sample at the reference temperature, T °C (20 °C in this work) and σ_θ is the measured conductivity at temperature, θ °C, and α is a temperature coefficient for the concrete (°C^{-1}). Regarding the temperature coefficient, the α value for concrete in both saturated and partially saturated states was taken as 0.035 °C^{-1} [17]. As an example, Fig. 2 presents the variation of as-measured conductivity, standardised conductivity and concrete-cover temperature for the marine-site specimens (exposure XS1, at a depth of 10 mm).

The as-measured conductivity values should not be discarded and it is important to use both standardised and as-measured data. The standardised values will assist in distinguishing between changes in conductivity due to temperature and changes due to the coupled effects of ionic ingress and changing levels of saturation. If conductivity/resistivity is to be used as a parameter in the assessment of corrosion rate (see Table 3 [19]), then it is the as-measured value that will be of more significance. As the temperature of the concrete decreases, not only will its conductivity decrease, but the anodic and cathodic reaction rates associated with a corrosion

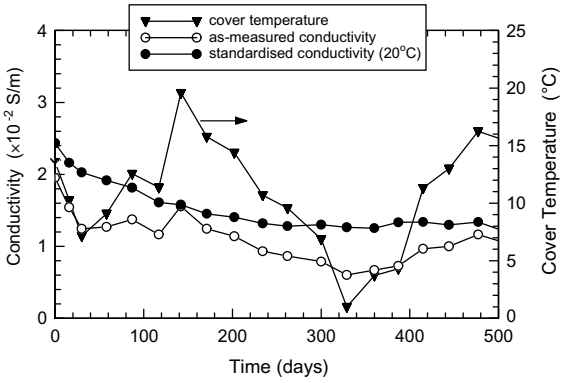

Fig. 2. Temperature variation within the covercrete for samples placed at marine site (PC sample: high-level location, at a depth of 10 mm from the exposed surface). The as-measured conductivity and standardised conductivity are also presented.

Table 3
Empirical resistivity/conductivity thresholds for depassivated steel reinforcement [19]

Resistivity (Ωm)	Conductivity (S/m)	Probable corrosion rate
<50	$>2\times10^{-2}$	Very high
50–100	2×10^{-2}–10^{-2}	High
100–200	10^{-2}–5×10^{-3}	Low to moderate
>200	$<5\times10^{-3}$	Low

cell would also be reduced—i.e. the corrosion process will be slower at the lower temperature.

4.2. Marine exposure site

4.2.1. High-level (XS1)

At this location, samples were not subjected to tidal action hence changes within the cover-zone will reflect the influence of ambient weather conditions and airborne spray. Although measurements were taken at all ten electrodes pairs positioned within the covercrete, for clarity, Figs. 3(a)–(c) present the conductivity versus time response from electrodes positioned at 5, 10, 15, 30 and 50 mm from the exposed surface for, respectively, the PC, GGBS and PFA specimens. It is evident that the electrodes positioned within the surface 5–15 mm display a more erratic response over the initial two months than those at greater depths within the covercrete. After this time, the response from the plain PC specimens, at all depths, remains relatively constant over the test period presented. This would imply that for this exposure condition, the moisture (and ionic) condition within the samples must attain stability. Those specimens with replacement material display a more marked decrease at all depths, particularly the PFA concrete mix. The decrease in conductivity for the GGBS and PFA mixes relative to their initial value is attributed the on-going pozzolanic reaction which is slower than the hydration of Portland cement and, in the longer term, results in a finer, more tortuous and discontinuous pore network than plain Portland cement. The effect of the latter will result in a progressive, long-term decrease in conductivity.

At the end of the exposure period, the conductivity of the concrete (at 20 °C) at the depth of the reinforcement (i.e. 50 mm) is, ≈0.030 S/m (33 Ω m) for the plain PC blocks, 0.012 S/m (83 Ω m) for the GGBS blocks and 0.008 S/m (125 Ω m) for the PFA blocks.

4.2.2. Mid-level (XS3)

The mid-level blocks are just submerged at full-tide and results are presented in Figs. 4(a)–(c). Over the initial 3 months exposure, conductivity values in the

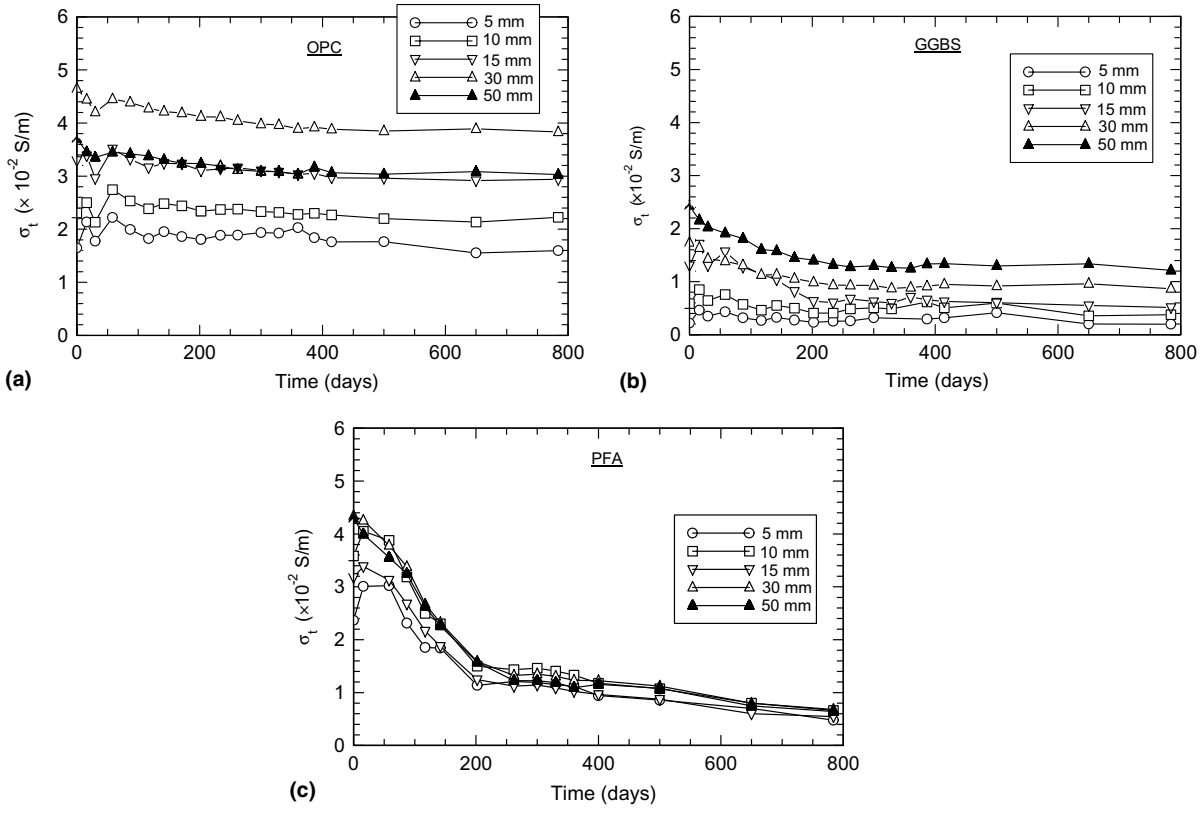

Fig. 3. Conductivity variation within the covercrete for (a) PC, (b) GGBS; and (c) PFA concrete, positioned at the high-level location.

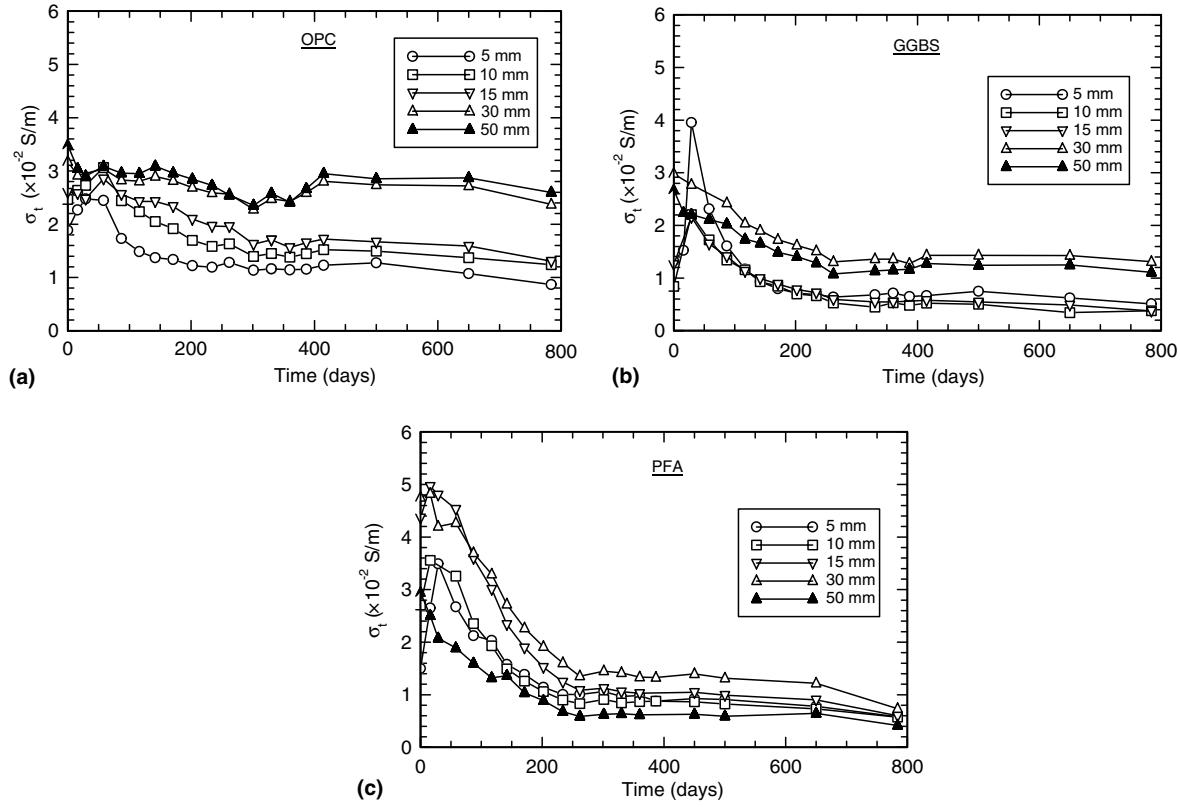

Fig. 4. Conductivity variation within the covercrete for (a) PC, (b) GGBS; and (c) PFA concrete, positioned at the mid-level location.

surface 5–15 mm increase in comparison to their high-level counterparts, in particular the GGBS and PFA mixes. This enhancement in conduction must be attributable to ionic ingress from tidal action. It is important to note that the conductivity will be a measure of the free ions in the pore fluid, as opposed to bound or immobile ions; it is the free chloride ions which are of significance in connection with corrosion of steel. Deeper levels (30 mm and 50 mm) do not display this response, instead they continually decrease with time. It is also apparent that after the initial 3 months, conductivity values for the surface electrodes reduce with time and, after approximately 12 months, display a more uniform behaviour. Generally, conductivity values at all depths within the cover-zone have decreased relative to their initial values. Regarding the latter, the responses suggest that, apart from the initial 3 months, microstructural changes within the surface 5–15 mm due to hydration, pozzolanic reaction and chloride binding are, at this stage, exerting a greater influence on conductivity values than changes in pore fluid chemistry due to ionic ingress from tidal action.

At the end of the exposure period, the conductivity (at 20 °C) of the concrete at 50 mm is, ≈0.025 S/m (40 Ω m) for the plain PC specimens, 0.011 S/m (91 Ω m) for the GGBS specimens and 0.006 S/m (160 Ω m) for the PFA specimens.

4.2.3. Low-level (XS2)

At this location the samples are positioned just above low water mark with the result that they are submerged during most of the tidal cycle. They are subjected to a maximum hydrostatic head of approximately 2.5 m at full-tide, increasing to approximately 3.5 m during spring tides. Figs. 5(a)–(c) present the conductivity versus time response for the specimens. Responses similar to the mid-level specimens are evident: an increase in conductivity within the surface 5–15 mm over the initial 2–3 months exposure, thereafter, values generally decrease with time although, at the end of the period presented, the conductivity of the PC specimens begins to display an increase over the surface 5 mm.

At the end of the exposure period, the conductivity (at 20 °C) of the concrete at 50 mm is, ≈0.02 S/m (50 Ω m) for the plain PC specimens, 0.012 S/m (83 Ω m) for the GGBS specimens and 0.01 S/m (100 Ω m) for the PFA specimens.

Fig. 6(a) presents the change in conductivity relative to the initial value for the PC specimens in Fig. 5(a) i.e. data are presented in the form of Eq. (2) above. This formalism gives a clearer picture as to whether the conductivity has increased or decreased relative to its value at the beginning of exposure. Where the conductivity shows a progressive increase, this would signify that increasing ionic concentration in the pore fluid, at that

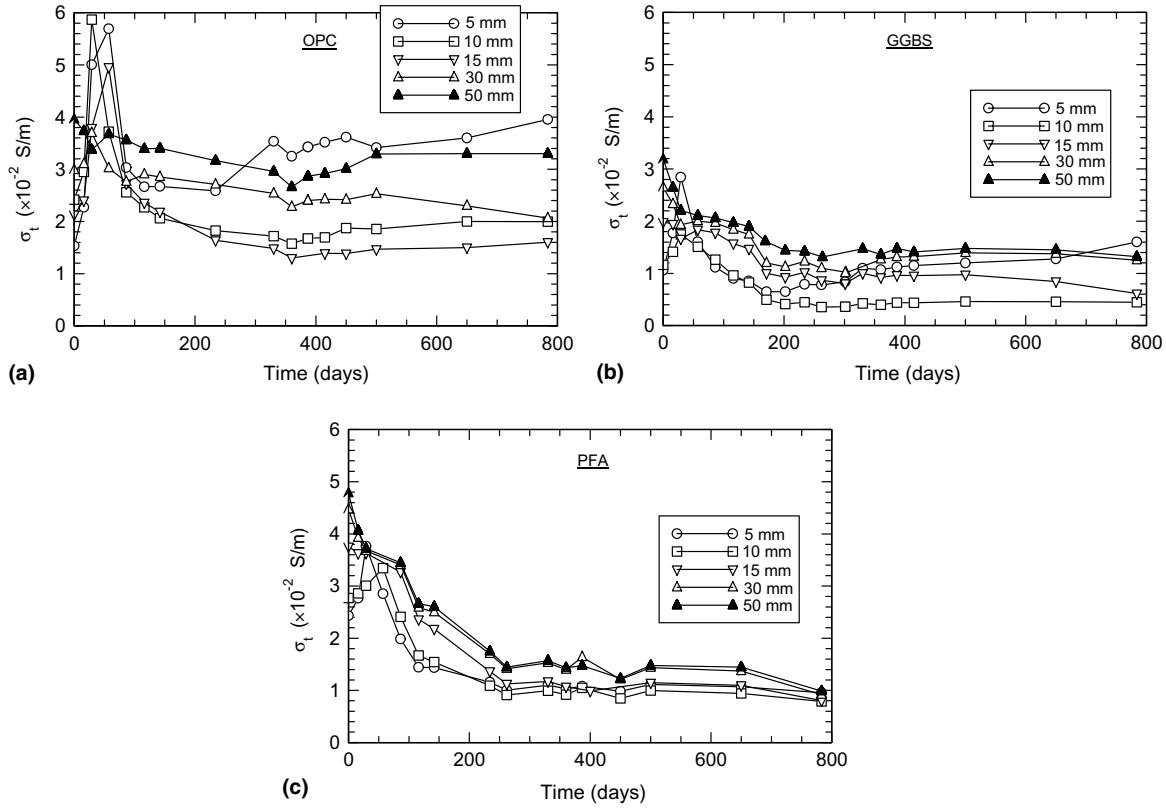

Fig. 5. Conductivity variation within the covercrete for (a) PC, (b) GGBS; and (c) PFA concrete, positioned at the low-level location.

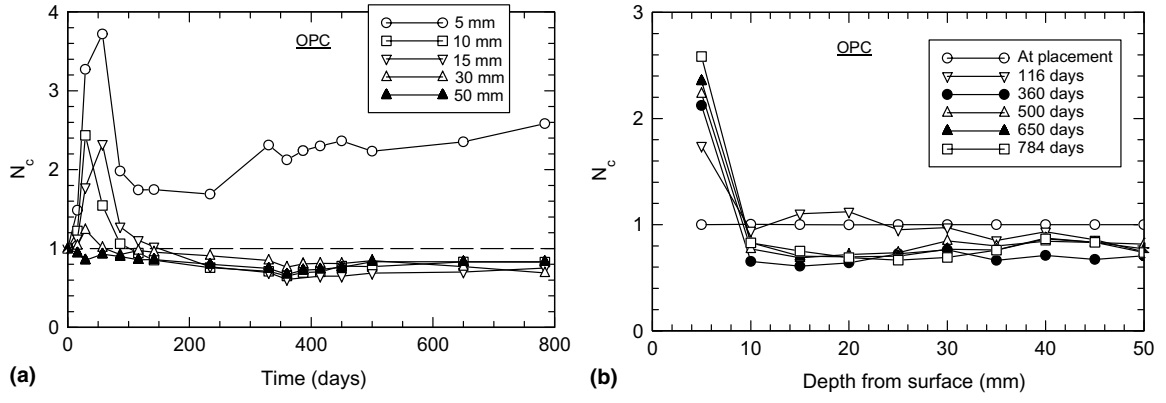

Fig. 6. PC concrete at low-level location: (a) normalised conductivity; and (b) change in normalised conductivity with depth through the cover-zone.

depth, dominates over pore structure refinement due to hydration, pozzolanic reaction and chloride binding effects, the latter reducing the conductivity of the concrete. In the longer term, therefore, as the influence of hydration diminishes, the conductivity will be dominated by the conductivity of the pore fluid. From Fig. 6(a), it is evident that the surface 5 mm of the cover displays a marked increase and indicates the extent of ionic penetration into the surface zone.

Normalised conductivity, N_c, versus depth profiles for the PC specimens are presented in Fig. 6(b) at selected times over the test period. These plots further highlight the influence of ionic ingress into the covercrete as there is a gradual enhancement in conductivity over the surface 5 mm or so. At deeper levels the conductivity values attain a relatively uniform value after the first 200 days of the test. It is anticipated that as the ions advance through the covercrete, each electrode

depth on the array will, in sequence, display a conductivity value increasing with time.

4.3. Urban exposure site (XC4/XF1)

Figs. 7(a)–(c) present the conductivity versus time curves for the plain PC, GGBS and PFA specimens respectively. Prior to being outside, electrode-pairs at all positions display a decrease in conductivity, indicative of a combined effect of drying, on-going hydration and pozzolanic reaction. After being placed outside (during a period of rain), the electrodes within the surface 5–15 mm display an immediate increase in conductivity eventually settling to a conductivity value greater than that before being placed outside. Those electrodes positioned within the surface 5–15 mm are thus influenced by the extended period of drying in the laboratory. Electrodes positioned at 50 mm continue to decrease over the period and would imply that they are sufficiently removed from the influence of surface drying effects and will, in the main, reflect hydration and pozzolanic reaction.

At the end of the exposure period, the conductivity (at 20 °C) of the concrete at 50 mm is, ≈0.025 S/m (40 Ω m) for the plain PC specimens, 0.015 S/m (67 Ω m) for the GGBS specimens and 0.006 S/m (167 Ω m) for the PFA specimens.

For illustrative purposes, Fig. 7(d) presents the normalised conductivity results for the data presented in Fig. 7(a) for PC concrete. Two features of the response are evident (and observed on all concretes):

1. On wetting, electrodes positioned at 30 mm and 50 mm display a reduction in conductivity, before increasing to values similar to those before wetting over the following 2 weeks. As the water-front moves into the partially saturated surface zone, it must 'push' a volume of air ahead of it which disperses into the pore network. Since air could be regarded as non-conductive, this would have the transitory effect of reducing conductivity. The slower, diffusive movement of water into the covercrete then results in the conductivity at these depths increasing to values similar to that before placement.
2. After the initial increase in conductivity, values in the surface 5–15 mm reduce over the next 2–3 weeks, attaining stability after this time (not dissimilar to the high-level specimens at the marine site). The reduction would be due to further hydration stimulated by the ingress of water.

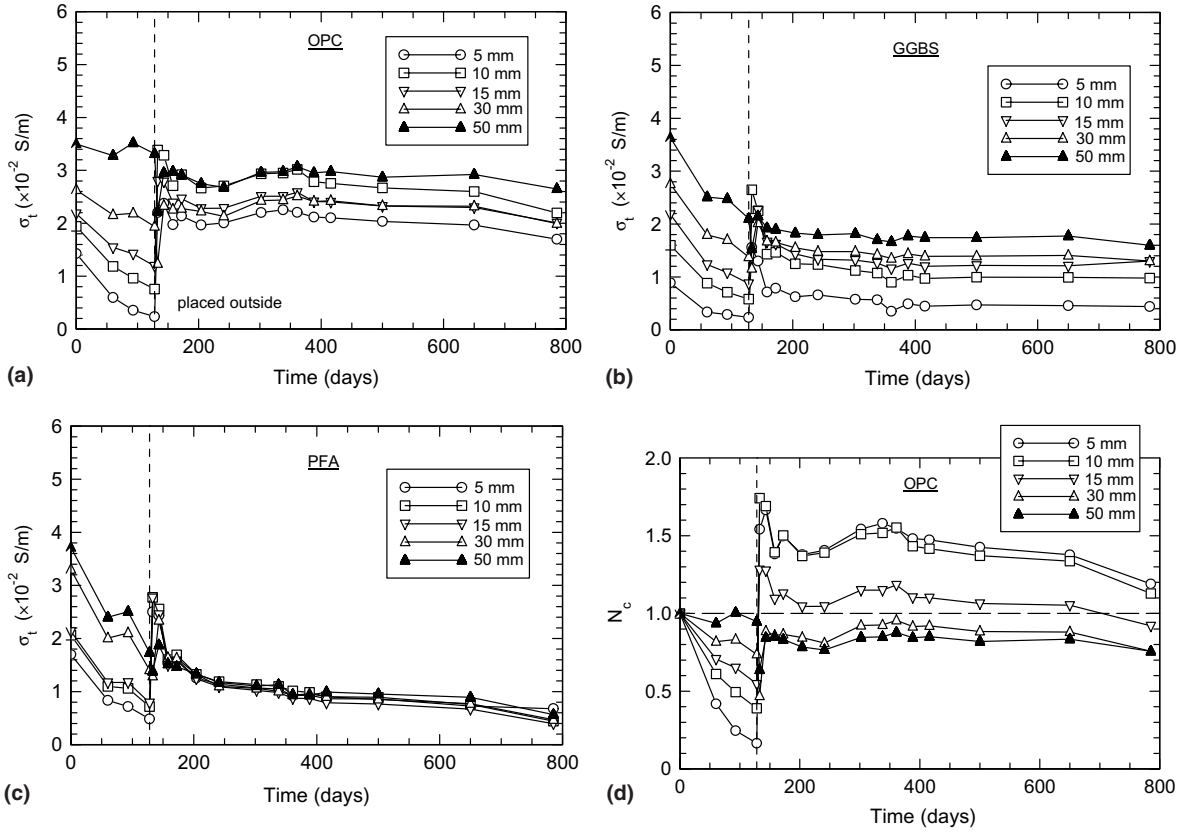

Fig. 7. Conductivity variation within the covercrete for (a) PC, (b) GGBS; (c) PFA concrete, positioned at the urban site; and (d) change in normalised conductivity for the PC concrete.

Generally, the results indicate that the surface 5–15 mm represents that part of the cover-zone most influence by prolonged drying effects at the surface. Since water moves rapidly through this zone its is not contributing to the protective qualities of the cover and, in such circumstances, could be regarded as 'lost cover'.

5. Concluding comment

A sensor system, which allows discretised electrical measurements within the covercrete, was utilised to study both the short- and long-term depth-related response of the covercrete subjected to a range of exposure conditions. The system can provide information on the electrical conductivity of concrete through the cover-zone, this parameter being important once the steel is depassified. The work has also highlighted the importance of regular monitoring of the covercrete as its properties change with time and depth; for example, the work clearly shows the pore structure refinement in blended cements during the post-curing period. Further work is required to ascertain the exact relationship between conductivity and ionic transport.

Acknowledgements

The work presented forms part of the concrete durability programme undertaken for the Scottish Executive Development Department (SEDD). Funding from the SEDD is gratefully acknowledged. The authors are also indebted to Highland Regional Council (now the North West Partnership) and McKay and McLeod (of Evanton) for their assistance and co-operation in setting up the marine site.

The views expressed in this paper are those of the authors and not necessarily those of the SEDD.

References

[1] McCarter WJ, Emerson M, Ezirim H. Properties of concrete in the cover zone: developments in monitoring techniques. Mag Conc Res 1995;47(172):243–51.

[2] Chrisp TM, McCarter WJ, Starrs G, Basheer PAM, Blewett J. Depth related variation in conductivity to study wetting and drying of cover-zone concrete. Cem Conc Comp 2002;24(5):415–27.

[3] Smart Structures: integrated monitoring systems for durability assessment of concrete structures. FORCE Institute (Denmark) Newsletter, No. 1. April, 2000. p. 1–2.

[4] Doran D. New standard for service-life planning. Struct. Eng. 2000;78(19):8.

[5] British Standards Institution, BS ISO 15686-1: 2000. Buildings and Constructed Assets. Service Life Planning. Part 1: General Principles. London.

[6] Schießl P, Raupach M. Monitoring corrosion risk in concrete structures—review of 10 years experience and new developments. In: Proceedings of 5th CANMET/ACI international conference on durability of concrete, Barcelona, SP-192, vol. 1. June 2000. p. 19–34.

[7] European Union—Brite EuRam III. Duracrete—Modelling of degradation. Report BE95-1347/R4-5. December 1998. 174pp (ISBN 90 376 0444 7).

[8] European Union—Brite EuRam III. Duracrete—Models for environmental actions on concrete structures' Report BE95-1347/R3. March 1999. 273pp (ISBN 90 376 0400 5).

[9] European Committee for Standardization (CEN), EN 206-1: 2000. Concrete—Part 1: Specification, Performance, Production and Conformity. Brussels.

[10] Schießl P, Raupach M. Instrumentation of Structures with Sensors—Why and How? In: Dhir RK, Jones MR, editors. Proceedings of concrete in the service of mankind conference, E&FN Spon, London. June 1996. p. 1–15.

[11] Schießl P, Raupach M. New approaches for monitoring the corrosion risk for the reinforcement—installation of sensors. In: Proceedings of concrete across borders conference, Odense, Denmark, vol. 1. 1994. p. 65–77.

[12] European Committee for Standardization (CEN), EN 197-1: 2000. Cement—Part 1: Composition, specifications and conformity criteria for common cements. Brussels.

[13] British Standards Institution, BS3892-1. Pulverised-fuel ash. Part 1. Specification for pulverised-fuel ash for use with Portland cement. London: 1997.

[14] British Standards Institution, BS6699. Specification for ground granulated blastfurnace slag for use with Portland cement. London; 1992.

[15] McCarter WJ, Brousseau R. The AC response of hardened cement paste. Cem Conc Res 1990;20(6):891–900.

[16] Gowers KR, Millard SG. Measurement of concrete resistivity for assessment of corrosion severity of steel using Wenner technique. Am Conc Inst Mater J 1999;96(5):536–41.

[17] Chrisp TM, Starrs G, McCarter WJ, Rouchotas E, Blewett J. Temperature–conductivity relationships for concrete: and activation energy approach. J Mater Sci Lett 2001;20(12):1085–7.

[18] Castellote M, Andrade C, Alonso MC. Standardization, to a reference temperature of 25 °C, of electrical resistivity for mortars and concretes in saturated or isolated conditions. Am Conc Inst Mater J 2002;99(2):119–28.

[19] Broomfield JP. Corrosion of steel in concrete. E&FN Spon; London: 1997. 240pp (ISBN 0 419 19630 7).